

# IF-GAN: A Novel Generator Architecture with Information Feedback

Seung Park<sup>a</sup>, Yong-Goo Shin<sup>b,\*</sup>

<sup>a</sup>Biomedical Engineering, Chungbuk National University Hospital, 776, Seowon-gu, Cheongju-si, Chungcheongbuk-do, Rep. of Korea

<sup>b</sup>Department of Artificial Intelligence, Hannam University, Daedeok-Gu, Daejeon, 34430, Rep. of Korea

## ARTICLE INFO

**Keywords:**  
Generative adversarial networks  
Image generation  
Information Feedback  
Gating module

## ABSTRACT

This paper presents an alternative generator architecture for image generation, having a novel information feedback system. Contrary to conventional methods in which the latent space unilaterally affects the feature space in the generator, the proposed method trains not only the feature space but also the latent one by interchanging their information. To this end, we introduce a novel module, called information feedback (IF) block, which jointly updates the latent and feature spaces. To show the superiority of the proposed method, we present extensive experiments on various datasets including subsets of LSUN and FFHQ. Experimental results reveal that the proposed method can dramatically improve the image generation performance, in terms of Frechet inception distance (FID), kernel inception distance (KID), and Precision and Recall (P & R).

## 1. Introduction

The generative model aims to synthesize complex real-world data distributions from random vectors sampled from prior distributions. The existing generative models can be roughly divided into three groups [5]: autoregressive models [28, 43], variational auto encoders (VAE) [19], and generative adversarial networks (GANs) [7]. Between these generative models, GANs-based ones have achieved impressive results in various fields including image generation [16, 15, 26, 54], text-to-image translation [34, 10], image-to-image translation [12, 6, 55], and image inpainting [51, 37, 41]. Following this trend, this paper aims to investigate and further develop the GANs-based generative model.

In general, the GANs-based image generation technique produces random images from a target dataset, given only access to an initial set of training images [22]. To achieve this goal, two different networks, *i.e.*, generator and discriminator, are trained simultaneously, but their objective functions are opposed to each other. Specifically, the discriminator is trained to classify the input as either a real image or a fake one, whereas the generator is trained to produce the fake image that the discriminator cannot distinguish. That means the generator and discriminator compete with each other to minimize their own objective functions. Theoretically, given enough data and model capacity, the generator is converged to produce the real data distribution [7, 22]. However, since the competition between the generator and discriminator is held in the high-dimensional feature space, the training procedure of GANs is unstable and often fails. Thus, it is hard to observe the ideal situation where the generator synthesizes the target real samples perfectly.

To alleviate this problem, extensive studies have been carried out. Some papers [47, 26, 8, 20, 53] noticed that the sharp gradient space of the discriminator gives rise

to the unstable GANs training. Thus, to prevent the discriminator from making sharp gradients, various regularization [53, 54, 25, 35] and normalization techniques [26, 22] have been proposed. More specifically, existing papers [8, 46, 45, 20, 36] usually add the regularization term, which constrains the magnitude of the gradient space, into the objective functions. For example, some papers [8, 46, 45] employed the regularization term, called gradient penalty, which use the magnitude of the gradient space as the penalty term. As the normalization strategy, spectral normalization (SN) [26], which normalizes the Lipschitz constant around one, is widely used in recent studies [49, 48, 33]. These regularization or normalization techniques are effective to improve the GAN performance, but the instability problem in the GAN training is still left.

To boost the GANs performance, some papers proposed generator or discriminator architectures with a novel deep learning modules [27, 49, 29, 33, 48, 30]. Miyato *et al.* [27] introduced a conditional projection technique that effectively provides the conditional information to the discriminator. Yeo *et al.* [49] proposed a cascading rejection module which iteratively classifies real and generated images by making orthogonal features. Recently, Park *et al.* [29] proposed a novel residual blocks which contains an additional side-residual path. Furthermore, Park *et al.* [33] developed a novel residual shortcut module, called gating shortcut, which remains (or remove) the meaningful feature (or unnecessary feature) via the residual shortcut. In recent, Yeo *et al.* [48] proposed a novel normalization technique that conducts the region adaptive affine transformation.

On the other hand, there are some attempts [32, 38, 31, 17] to modulate the convolutional kernel to improve the GANs performance. Park *et al.* [32] introduced a perturbed convolution (PConv), which is designed to prevent the discriminator from overfitting problem. Sagong *et al.* [38] proposed conditional convolution, called cConv, which provides conditional information to the generator by scaling and shifting the weight matrix following the given condition. This

\*Corresponding author

✉ spark.cbnuh@gmail.com (S. Park); ygshin@hnu.kr (Y. Shin)  
ORCID(s):

method can improve the conditional GANs (cGANs) performance well, but it can be used only for the cGAN scheme not the unconditional image generation task. Recently, Park *et al.* [31] proposed a latent-adaptive convolution technique called GConv, which modulates the convolutional kernel following the given latent vector. This approach shows better performance than standard convolution technique in both GANs and cGANs schemes.

Traditionally, the generator uses the vector sampled from the latent space, *i.e.* random noise vector, as the input to the initial layer. In this paper, we will refer to this generator as a traditional generator. However, the traditional generator has a drawback in which it is difficult to generate a high-resolution image. To address this problem, some studies employed novel training skills, such as progressive growing [14] or skip connection [13], to the traditional generator, and showed that these training skills effectively lead the generator to produce the high-resolution image. To further enhance the generalization capability of the generator, Karras *et al.* [17] introduced a novel weight modulating technique, called StyleGAN, which scales the weight matrix using the value derived from the latent space. More specifically, StyleGAN utilized a nonlinear mapping network to project a random noise vector to a higher dimensional latent space, and the resulting vector is injected into different blocks of a generator to control the data generation process [5]. Since this method shows fine performance, many recent studies [17, 52, 15, 44] have explored various techniques while setting StyleGAN as their baseline model. Although recent StyleGAN-based generative models have shown notable performance, research to newly design the generator architecture is still in progress.

This paper mainly focuses on developing a novel generator architecture that significantly improves the GANs performance. Contrary to the ongoing studies that set the StyleGAN as their baseline model, we propose a novel generative model that handles the latent space in a different way. In the conventional methods including the traditional generator and StyleGAN, the latent space unilaterally affects the feature space in the generator. That means the information in the latent space is provided to the generator in a one-way. For instance, in StyleGAN, the nonlinear mapping network produces information without considering the current status of the image generation process. Here, we have pondered upon whether this approach is the best way to handle the latent space; we believe that there could be more effective way to deal with the latent space.

This paper investigates a generator architecture containing an information feedback system, which is named information feedback GANs (IF-GANs). In contrast with existing generative models, the proposed method not only trains the feature space in the generator but also reforms the latent space using the information in the feature space. To this end, we introduce a novel module, called information feedback (IF) block, which jointly updates the latent and feature spaces by interchanging their information. In order

to prove the superiority of the proposed method, we conducted experiments on various subsets of LSUN and FFHQ datasets. Quantitative evaluations show that the proposed method can improve the image generation performance, in terms of Frechet inception distance (FID) [9], kernel inception distance (KID) [2], and Precision and Recall (P & R) [21, 39]. In the remainder of this paper, we explain the background and preliminaries in Section 2 and introduce the proposed method in Section 3. In Section 4, extensive experimental results are presented to show the superior performance of the proposed method compared to conventional ones, and Section 5 concludes the paper.

The main contributions of this paper are described as follows:

- We propose a novel generative model, named IF-GANs, which shows impressive image generation performance.
- We design an architectural module called IF block, which is suitable for jointly training the feature and latent spaces, further substantially benefiting the image generation performance.
- We prove the feasibility of a novel generator framework, which is not attempted in the previous studies. To this end, we conduct extensive experiments on various subsets of LSUN and FFHQ datasets. In addition, we show that the proposed method achieves the remarkable performance with various quantitative evaluation metrics including FID, KID, and P & R.

## 2. Background and Preliminaries

### 2.1. Generative Adversarial Networks

In the training procedure of GANs [7], the generator  $G$  is trained to produce samples following the real data distribution  $P_{data}(x)$  and the discriminator  $D$  is optimized to classify the generated real and generated samples. The objective functions of  $D$  and  $G$  are defined as

$$L_D = -E_{x \sim P_{data}(x)}[\log D(x)] - E_{z \sim P_z(z)}[\log(1 - D(G(z)))] \quad (1)$$

$$L_G = -E_{z \sim P_z(z)}[\log(D(G(z)))] \quad (2)$$

where  $x$  indicates a sample from  $P_{data}(x)$  and  $z$  means a latent vector sampled from latent space  $P_z(z)$  such as Gaussian normal distribution. By minimizing these formulas,  $G$  could synthesize  $P_{data}(x)$  successfully if  $D$  is trained optimally. However, owing to various issues such as the gradient vanishing problem, the above formula often causes the training failure. To moderate this problem, many studies have reformulated Eqs. 1 and 2. For instance, Mao *et al.* [24] introduced a objective function based on least square error (LSGAN) and Arjovsky *et al.* [1] used Wasserstein distance to their objective function (WGAN). The current

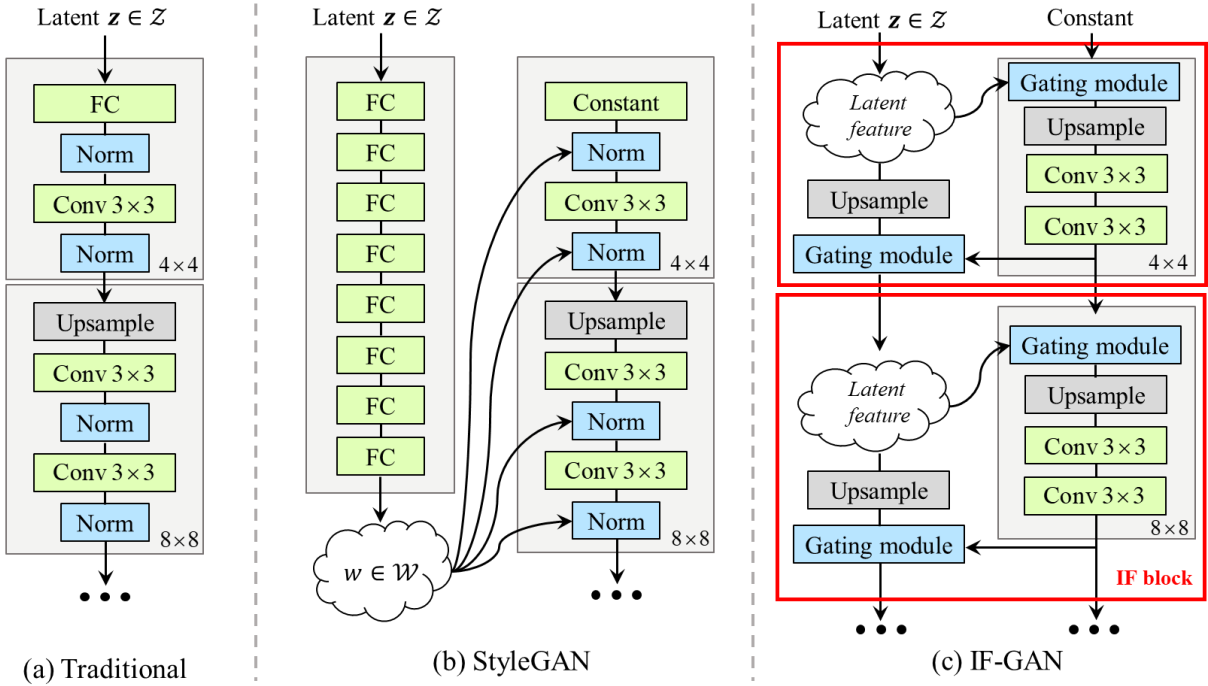


**Figure 1:** Comparison of the generator architectures. (a) The traditional generator that employs the latent space  $Z$  at the initial stage, (b) StyleGAN-based generator that builds the intermediate latent space  $W$  using the given latent space  $Z$  and mapping network, (c) The proposed generator that updates the latent space and the generator by sharing their information in the IF block (red box).

widely-used objective functions are hinge loss [3, 49, 27, 26, 32, 37, 41, 4] and non-saturating logistic loss with  $R_1$  regularization [25, 17, 16, 15]. More specifically, the non-saturating logistic loss with  $R_1$  regularization is formulated as follow:

$$L_D = E_{x \sim P_{\text{data}}(x)}[\log(1 + e^{-D(x)}) + \frac{\gamma}{2} \|\nabla D(x)\|^2] + E_{z \sim P_z(z)}[\log(1 + e^{D(G(z))})], \quad (3)$$

$$L_G = E_{z \sim P_z(z)}[\log(1 + e^{-D(G(z))})], \quad (4)$$

where  $\gamma$  is a hyper-parameter that constrains the gradient magnitude of the discriminator. In our experiments, we used Eqs. 3 and 4 to train the GANs.

## 2.2. Conventional Generator Architectures

In this paper, we categorize existing generator architectures into two different groups: traditional generator and StyleGAN-based generator. As shown in Figs. 1(a) and (b), the traditional generator uses the given latent space  $Z$  at the initial stage, whereas StyleGAN-based generator maps the  $Z$  to intermediate latent space  $W$ , and uses  $W$  to the image generation process. We agree that there are many recent works [17, 15, 29, 33, 52, 3] that modify the generator architecture, but they still use  $Z$  at the beginning of the generator [33, 3, 29] or build  $W$  [17, 52, 15] like StyleGAN.

Here we pinpoint the problem with the conventional approaches that latent feature, *i.e.* the feature obtained from the latent space, is first built in the initial stage, without reflecting on the feature of the image to be generated (image feature). For instance, the StyleGAN-based generator produces  $W$  using multiple fully-connected layers, and uses  $W$  to the image generation task. It is worth noting that  $W$  affects the image generation task, but not vice versa. That means the image feature cannot modulate  $W$  to be more conducive to the image generation task. Based on these observations, we hypothesize that the GANs performance could be further improved if latent features are updated by considering the image generation process. To prove our hypothesis, we proposed a novel generator architecture that not only trains the image feature but also modulates the latent one, by considering each other.

## 3. Proposed Method

The overall architecture of the proposed method, which consists of multiple IF blocks, is depicted in Fig. 1(c). In the remainder of this section, we will first introduce the IF block that is a core of the proposed method, and then present the deep learning module, *i.e.* gating module, used at the IF block.

### 3.1. Information Feedback Block (IF Block)

As illustrated in Fig. 2, the IF block consists of two different branches: latent branch (green box in Fig. 2) and

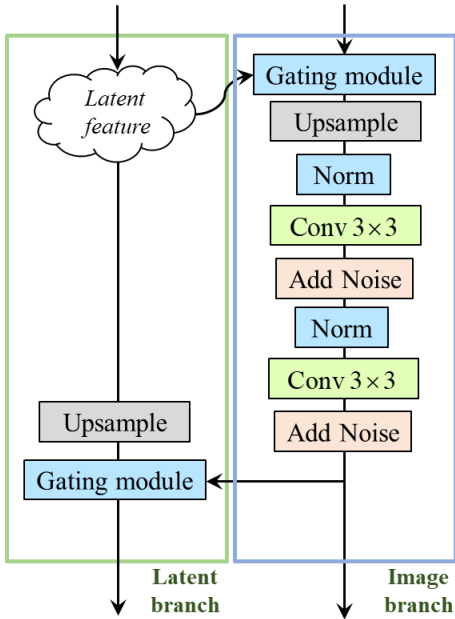


**Figure 2:** The illustration of the IF block. The IF block consists of the latent and image branches, and both branches share their information by using the gating module.

image branch (blue box in Fig. 2). In this paper, we will refer to the feature from each branch as the latent feature and image feature, respectively. To jointly update latent and image features, we design the IF block to make the latent and image branches alternately send and receive information. More specifically, the latent branch first provides the latent feature to the image branch via a gating module that effectively combines the features from the two different branches using the gating mechanism. The detailed architecture of the gating module will be explained in the next subsection. After integrating the latent feature and image feature using the gating module, the integrated features are updated using multiple normalization layers followed by ReLU function and convolution layers. In the IF block, as a normalization, we employ the modified batch normalization (BN) [3] technique that infers affine transformation parameters of the batch normalization using the noise vector. In addition, we use the noise addition technique introduced in [16], which adds per-pixel noise after each convolution layer to provide stochastic variation. The reader is encouraged to review the mentioned papers [3, 16] for more details. After that, using another gating module, we update the latent feature using the output of the image branch.

The major difference between the conventional generators and the proposed one is that the image feature affects the latent feature. More specifically, at the initial stage of the IF block, the latent feature is provided to the image branch. In addition, similar to the feedback system in which the output of a system is circled back and used as the input, the output of the image branch distributes the information to the latent feature used as the input of the image branch. That means the input latent feature gets feedback to become

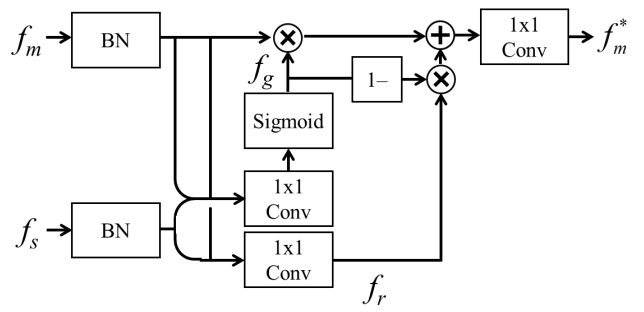


**Figure 3:** The illustration of the gating module. In the gating module, based on the gating mechanism,  $f_m^*$  is refined by using the  $f_s$ .

a more proper feature to the image branch; the updated latent feature can present meaningful information to the image branch in the next IF block. Note that this modification in the information flow leads to significant performance improvement. We will show the detailed explanations with ablation studies in Section 4.2.

### 3.2. Gating module

In our recent study [33], the capability of the gating module in the GANs scheme has been proved. Following this work, we apply the gating module to effectively blend two different features, latent and image features. As shown in Fig. 3, the gating module gets two different inputs, the main feature  $f_m$  and the side feature  $f_s$ . Specifically,  $f_m$  is a feature whose information will be retained or removed through the gating operation, whereas  $f_s$  is a feature providing the information needed for  $f_m$  refinement. Therefore, at the gating module in the image branch, we use the image feature as  $f_m$  and the latent feature as  $f_s$ . In contrast, at the gating module in the latent branch, the latent feature is utilized as  $f_m$  and the image feature as  $f_s$ .

The detailed process in the gating module is as follows: First, since  $f_m$  and  $f_s$  have different scales, we use the BN [11] to balance the scales of them. Then, we produce the gate feature  $f_g$  using a convolutional layer having the sigmoid function as the activation function. This procedure can be formulated as follows:

$$f_g = \sigma[\text{Conv}(f_m \odot f_s)], \quad (5)$$

where  $\text{Conv}$  and  $\odot$  indicate the  $1 \times 1$  convolution layer and channel concatenation operation, respectively, whereas  $\sigma$  means the sigmoid function. In addition, we produce the refinement feature  $f_r$ , which will be combined with  $f_m$ , in a similar manner, as shown below:

$$f_r = \text{Conv}(f_m \odot f_s). \quad (6)$$

After that, by using  $f_g$  and  $f_r$ , we produce the output of the gating module,  $f_m^*$ , as follows:

$$f_m^* = \text{Conv}[f_g \otimes f_m + (1 - f_g) \otimes f_r], \quad (7)$$

where  $\otimes$  is the element-wise multiplication operation. Here, Eq. 7 can be interpreted as follows: the first term  $f_g \otimes f_m$  means what information needs to be retained in the  $f_m$ . In addition, the second term  $(1 - f_g) \otimes f_r$ , indicates that  $f_m$  is updated by using the refined information  $f_r$  which contains the information coming from  $f_s$ . That means, by using Eq. 7, the gating module learns how to effectively blend the information in two different features, *i.e.*  $f_m$  and  $f_s$ . Note that this paper does not intend to design an optimal gating module for the IF block; another module could be designed to achieve better performance. Instead of newly designing the gating module, this paper cares more about whether it is possible to boost the GANs performance by training the latent and image features together.

## 4. Experiments

### 4.1. Implementation Details

**Dataset** To show the effectiveness of the proposed method, we performed experiments on the FFHQ [16] and various classes in LSUN [50], *i.e.* church, bed, and car. The resolution of images are resized to  $128 \times 128$  and  $256 \times 256$  pixels.

**Network Architecture** The goal of this paper is to show the effectiveness of the novel generator architecture. Thus, for a fair comparison, we compared the performance of existing generators and the proposed one in the same environment. Toward this end, in all our experiments, we used the common discriminator which follows the discriminator architecture of StyleGAN-v2 [17]. Specifically, the discriminator consists of multiple residual blocks using leaky ReLU [23] with  $\alpha = 0.2$  as the activation function. More detailed architecture of the discriminator is explained in [17].

On the other hand, we implemented the traditional and proposed generator architectures as follows: For building the StlyeGAN-based generator, we used the official *Pytorch* implementation of StyleGAN-v2 paper [17]. In contrast, we implemented the traditional generator by stacking up the multiple residual blocks following the previous papers [26, 3, 33] but did not use spectral normalization in the generator. We also implemented the proposed method by stacking up the multiple IF blocks. The detailed architecture of the proposed method and feature dimensions are summarized in Table 1. In summary, we built the StlyeGAN-based generator using the official code, whereas we implemented the traditional generator and proposed method. Note that for a fair comparison, we adjusted the hyperparameters of the official StlyeGAN-v2 source code to match the number of feature dimensions in each resolution with the proposed method. Since our experiments use a smaller number of feature dimensions than the original StlyeGAN-v2 generator, it showed poor performance compared to its original performance. We will further explain the reason for the performance degradation and the validity of the experiments in Sec. 4.2.

**Table 1**

Network architectures of the generator and discriminator for  $128 \times 128$  (top) and  $256 \times 256$  (bottom) images.

Generator	Discriminator
$z \in \mathbb{R}^{32} \sim N(0, I)$	RGB image
FC, $4 \times 4 \times 512$	$1 \times 1$ Conv, 64
IF block, 512	ResBlock, down, 64
IF block, 512	ResBlock, down, 128
IF block, 256	ResBlock, down, 256
IF block, 128	ResBlock, down, 512
IF block, 64	ResBlock, down, 512
BN, ReLU	Mini-batch Std
$1 \times 1$ Conv, Tanh	Dense, 512
	Dense, 1

Generator	Discriminator
$z \in \mathbb{R}^{32} \sim N(0, I)$	RGB image
FC, $4 \times 4 \times 512$	$1 \times 1$ Conv, 32
IF block, 512	ResBlock, down, 32
IF block, 512	ResBlock, down, 64
IF block, 256	ResBlock, down, 128
IF block, 128	ResBlock, down, 256
IF block, 64	ResBlock, down, 512
IF block, 32	ResBlock, down, 512
BN, ReLU	Mini-batch Std
$1 \times 1$ Conv, Tanh	Dense, 512
	Dense, 1

**Training Details** As mentioned in Sec. 2.1, we employed the non-saturating logistic loss with  $R_1$  regularization as the objective function where we set  $\gamma = 10$ . In addition, we used the Adam optimizer [18] with  $\beta_1 = 0.9$  and  $\beta_2 = 0.99$ . The batch size of the discriminator and generator are set to 32, and both networks are trained for 300k iterations. The learning rates of the generator and discriminator are set to 0.0025, where the learning rate decayed linearly over the last 50k iterations. In addition, we employed the lazy regularization technique [17] where  $R_1$  regularization is performed only once every 16 mini-batches. All models are trained on a single Nvidia RTX 3090 graphic processing unit (GPU).

**Evaluation Metrics.** In this paper, we employed the most popular metrics in the GANs scheme, FID [9], KID [40], and P&R [21, 39], which quantify how realistic the generated image is. In particular, the FID measures the Wasserstein-2 distance between the feature distributions of the real and generated images, which are obtained via the pre-trained Inception model [42]. On the other hand, the KID calculates the squared maximum mean discrepancy (MMD) between Inception representations. The generated samples with better quality have lower FID and KID scores. P&R quantify the percentage of generated images that are similar to training images and the percentage of training images that can be generated, respectively. In our experiments, we randomly

**Table 2**

Comparison of GAN performances between the traditional generator, StyleGAN-based generator, and the proposed method on FFHQ and LSUN datasets in terms of FID, KID, and P & R. We marked the lowest FID and KID scores in bold. In addition, we marked the scores with the highest sum of P and R in bold.

Dataset	Metrics	128 × 128 Resolution			256 × 256 Resolution		
		Traditional	StyleGAN	Proposed	Traditional	StyleGAN	Proposed
FFHQ	FID	5.70	7.38	<b>5.07</b>	6.54	6.83	<b>5.41</b>
	KID	0.0024	0.0028	<b>0.0020</b>	0.0027	0.0024	<b>0.0019</b>
	P/R	0.67/0.42	0.68/0.28	<b>0.67/0.44</b>	0.67/0.41	0.70/0.30	<b>0.67/0.44</b>
Church	FID	4.73	6.68	<b>4.38</b>	5.42	6.43	<b>4.74</b>
	KID	0.0026	0.0040	<b>0.0024</b>	0.0030	0.0041	<b>0.0024</b>
	P/R	0.51/0.51	0.58/0.34	<b>0.51/0.53</b>	0.50/0.49	0.56/0.35	<b>0.51/0.48</b>
Bed	FID	7.82	8.58	<b>5.49</b>	7.71	8.50	<b>7.14</b>
	KID	0.0054	0.0060	<b>0.0029</b>	0.0052	0.0055	<b>0.0049</b>
	P/R	0.51/0.39	0.51/0.24	<b>0.50/0.42</b>	0.48/0.34	0.50/0.20	<b>0.52/0.34</b>
Car	FID	5.07	8.05	<b>4.09</b>	6.25	7.66	<b>5.05</b>
	KID	0.0019	0.0028	<b>0.0013</b>	0.0023	0.0030	<b>0.0017</b>
	P/R	0.58/0.42	0.64/0.19	<b>0.58/0.44</b>	0.57/0.38	0.62/0.21	<b>0.59/0.40</b>

**Table 3**

Performances of the proposed method when replacing the gating module with the simple mathematical operations on FFHQ and LSUN datasets in terms of FID, KID, and P & R.

Dataset	Sum			
	FID↓	KID↓	P	R
FFHQ	5.64	0.0026	0.66	0.43
Church	4.79	0.0028	0.52	0.52
Bed	7.41	0.0048	0.50	0.41
Car	4.87	0.0018	0.53	0.43

Dataset	Concatenation			
	FID↓	KID↓	P	R
FFHQ	5.08	0.0021	0.67	0.42
Church	4.55	0.0026	0.51	0.53
Bed	6.20	0.0041	0.53	0.40
Car	4.50	0.0015	0.59	0.44

generated 50,000 samples and computed the metrics. In addition, for a fair comparison, we measured the FID, KID, and P&R performances of the traditional, StyleGAN-based, and the proposed generative models, using the official *Pytorch* code introduced in [17].

## 4.2. Experimental Results

**Quantitative Results** To highlight the superiority of the proposed method, we measured the GANs performance on various datasets such as FFHQ and subsets of LSUN. Indeed, since this paper presented a novel framework of the generative model, it is a little difficult to compare the GAN performance with specific algorithms. Therefore, we compared the performance of the proposed method with the popular baseline models referred to as the traditional generator and StyleGAN-based generator. Table 2 shows the

**Table 4**

Performances of the proposed method when removing the gating module in the latent branch on FFHQ and LSUN datasets in terms of FID, KID, and P & R.

Dataset	FID↓	KID↓	P	R
FFHQ	5.90	0.0027	0.67	0.41
Church	4.56	0.0024	0.53	0.49
Bed	6.63	0.0042	0.49	0.42
Car	4.65	0.0017	0.58	0.44

experimental results. At first, we noticed the performances of the traditional generator and StyleGAN-based generator. In general, many studies have believed that the StyleGAN-based generator shows better performance than the traditional generator. However, in our experiments, the traditional generator showed better performance than the StyleGAN-based generator in all datasets. Owing to these experimental results, one may have doubts about the reliability of our experiments. Indeed, there are two main causes for these results: First, since we use a single GPU, we could not follow the original parameters setting, *e.g.* batch size and a number of feature dimensions, in the official StyleGAN-v2 code. Second, for a fair comparison with the proposed method, we used the training skills that improve the GAN performance, such as lazy regularization and noise addition presented in [16, 17], to the traditional generator. (The traditional generator usually employs the SN to both generator and discriminator, instead of using the  $R_1$  regularization technique.) Due to these reasons, this paper does not refer to the traditional generator and StyleGAN-based generator as the specific algorithms; this paper mainly focuses on presenting a novel framework of the generative model rather than improving the performance of a specific algorithm.

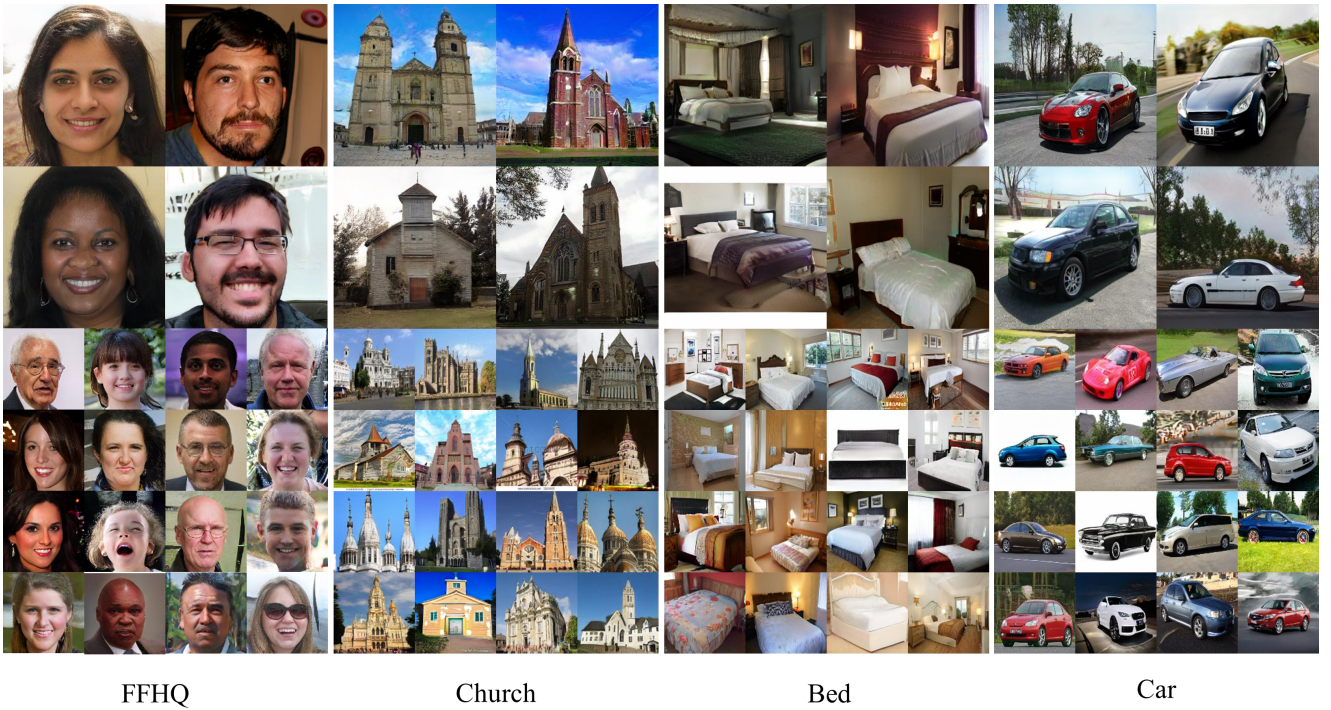


**Figure 4:** Samples of the generated images using the proposed method on FFHQ, LSUN-church, LSUN-Bed, and LSUN-Car. The top two rows are  $256 \times 256$  resolution images and the other rows are  $128 \times 128$  resolution images.

As shown in Table 2, the proposed method showed better FID and KID performances than the traditional generator. Here, we noted these results since they effectively revealed the superiority of the proposed method compared with the traditional generator. In our experiments, we utilized the same deep learning modules and training skills, such as modified BN [3], noise addition [16], and lazy regularization skill [17], for both traditional and proposed generators; the only difference between both models is whether to update the latent feature or not. That means the proposed generator achieved better performance than the traditional one by jointly updating the latent and image features. In addition, compared with the StyleGAN-based generator, our new design not only achieves lower FID and KID scores but also exhibits notable shift from precision to recall. As mentioned in [17, 21], these results are generally desirable since recall can be traded into precision via truncation, whereas the opposite is not true. Based on these results, we concluded that the proposed generative model is more effective to generate high-quality image compared with the existing approaches.

**Ablation Studies** Furthermore, to clearly show which part of the proposed method improves the GANs performance, we conducted ablation studies. At first, we checked the effectiveness of the gating module. Indeed, the features in the latent and image branches can be combined by using simple mathematical operations such as sum or concatenation. Thus, we conducted additional experiments that replace the gating module with sum and concatenation operations.

In our ablation studies, we set the resolution of all datasets as  $128 \times 128$ . As observed in Tables 2 and 3, the gating module in the proposed method showed better performance than the simple operations, especially in terms of FID and KID scores. We agree that there could be another module more suitable to combine features in two different branches. However, as mentioned in 3.2, this paper cares more about whether it is possible to improve the GANs performance by integrating those features. Instead, we noticed that the proposed method still exhibited comparable or better performance than the conventional generators, even if using simple mathematical operations including sum and concatenation.

On the other hand, we checked the effectiveness related to the joint training of latent and image features. Toward this end, we removed the gating module in the latent branch, which updates the latent feature using the image feature. That means, in this case, the latent feature affects the image feature, but not vice versa. Note that we do not conduct an ablation study about removing the gating module in the image branch, where the image feature is updated by using the latent feature, since if that gating module is removed, the latent branch cannot provide any information to the image branch. That means the latent branch is not used for the image generation task. In our experiments, the resolution of all datasets is set to  $128 \times 128$ , and the experimental results are summarized in Table 4. As shown in Tables 2 and 4, the proposed method without the gating module in the image branch showed poor performance, even compared with the traditional generator. That means the IF block is not useful when only updating the image feature; the

IF block is effective when training both image and latent features by interchanging their information. Based on these observations, we concluded that the GANs performance can be considerably boosted by jointly modulating the latent and image features even with a simple operation.

**Qualitative Results** Fig. 4 shows the sample images of the proposed method. Indeed, we agree that it is reasonable to compare the generated image quality of the conventional and the proposed methods. However, since random noise is used as the input to generate the images, it is difficult to fairly compare the image quality of conventional and proposed methods. Therefore, following the previous papers [3, 49, 33, 31], this paper only presents the generated images of the proposed method. As illustrated in Fig. 4, the proposed method produces visually pleasing image on the challenging datasets; the proposed method could synthesize the images with complex scenes.

**Limitations** Despite the significant improvements, the proposed method still faces one confusion, *i.e.* hardware efficiency. Since a single IF block contains the two gating modules consisting of multiple normalization and convolutional layers, it needs more computational costs than the existing method; the proposed method requires more GPU memory and computational time. However, as demonstrated in Table. 3, the proposed method still shows superior performance to conventional methods, even using simple mathematical operations instead of the gating module. Thus, in our future work, we will further investigate the simple but effective module which could alleviate the computational complexity of IF block.

## 5. Conclusion

We have presented a novel generative model, called IF-GAN, having the information feedback system which jointly updates the latent and image features. Toward this end, we have introduced a deep learning module called IF block that interchanges the information in the latent and feature spaces via the gating module. We have demonstrated the effectiveness of the proposed method by showing extensive experimental results. In addition, we have further investigated the validity of the proposed method in its broad aspects through ablation studies. Therefore, we believe that the proposed method is useful to various GAN-based image generation tasks.

## Declaration of Competing Interest

The authors declare no conflict of interest.

## References

- [1] Arjovsky, M., Chintala, S., Bottou, L., 2017. Wasserstein generative adversarial networks, in: International conference on machine learning, PMLR. pp. 214–223.
- [2] Bińkowski, M., Sutherland, D.J., Arbel, M., Gretton, A., 2018. Demystifying mmd gans. arXiv preprint arXiv:1801.01401 .
- [3] Brock, A., Donahue, J., Simonyan, K., 2018. Large scale gan training for high fidelity natural image synthesis. arXiv preprint arXiv:1809.11096 .
- [4] Chen, T., Zhai, X., Ritter, M., Lucic, M., Houlsby, N., 2019. Self-supervised gans via auxiliary rotation loss, in: Proceedings of the IEEE Conference on Computer Vision and Pattern Recognition, pp. 12154–12163.
- [5] Chen, T., Zhang, Y., Huo, X., Wu, S., Xu, Y., Wong, H.S., 2022. Sphericgan: Semi-supervised hyper-spherical generative adversarial networks for fine-grained image synthesis, in: Proceedings of the IEEE/CVF Conference on Computer Vision and Pattern Recognition, pp. 10001–10010.
- [6] Choi, Y., Choi, M., Kim, M., Ha, J.W., Kim, S., Choo, J., 2018. StarGAN: Unified generative adversarial networks for multi-domain image-to-image translation, in: Proceedings of the IEEE/CVF conference on computer vision and pattern recognition, pp. 8789–8797.
- [7] Goodfellow, I., Pouget-Abadie, J., Mirza, M., Xu, B., Warde-Farley, D., Ozair, S., Courville, A., Bengio, Y., 2014. Generative adversarial nets, in: Advances in neural information processing systems, pp. 2672–2680.
- [8] Gulrajani, I., Ahmed, F., Arjovsky, M., Dumoulin, V., Courville, A.C., 2017. Improved training of wasserstein gans. Advances in neural information processing systems 30.
- [9] Heusel, M., Ramsauer, H., Unterthiner, T., Nessler, B., Hochreiter, S., 2017. GANs trained by a two time-scale update rule converge to a local Nash equilibrium, in: Advances in Neural Information Processing Systems, pp. 6626–6637.
- [10] Hong, S., Yang, D., Choi, J., Lee, H., 2018. Inferring semantic layout for hierarchical text-to-image synthesis, in: Proceedings of the IEEE/CVF conference on computer vision and pattern recognition, pp. 7986–7994.
- [11] Ioffe, S., Szegedy, C., 2015. Batch normalization: Accelerating deep network training by reducing internal covariate shift, in: International conference on machine learning, PMLR. pp. 448–456.
- [12] Isola, P., Zhu, J.Y., Zhou, T., Efros, A.A., 2017. Image-to-image translation with conditional adversarial networks, in: Proceedings of the IEEE/CVF conference on computer vision and pattern recognition, pp. 1125–1134.
- [13] Karewar, A., Wang, O., 2020. Msg-gan: Multi-scale gradients for generative adversarial networks, in: Proceedings of the IEEE/CVF conference on computer vision and pattern recognition, pp. 7799–7808.
- [14] Karras, T., Aila, T., Laine, S., Lehtinen, J., 2017. Progressive growing of gans for improved quality, stability, and variation. arXiv preprint arXiv:1710.10196 .
- [15] Karras, T., Aittala, M., Laine, S., Härkönen, E., Hellsten, J., Lehtinen, J., Aila, T., 2021. Alias-free generative adversarial networks. Advances in Neural Information Processing Systems 34.
- [16] Karras, T., Laine, S., Aila, T., 2019. A style-based generator architecture for generative adversarial networks, in: Proceedings of the IEEE/CVF conference on computer vision and pattern recognition, pp. 4401–4410.
- [17] Karras, T., Laine, S., Aittala, M., Hellsten, J., Lehtinen, J., Aila, T., 2020. Analyzing and improving the image quality of stylegan, in: Proceedings of the IEEE/CVF conference on computer vision and pattern recognition, pp. 8110–8119.
- [18] Kingma, D.P., Ba, J., 2014. Adam: A method for stochastic optimization. arXiv preprint arXiv:1412.6980 .
- [19] Kingma, D.P., Welling, M., 2013. Auto-encoding variational bayes. arXiv preprint arXiv:1312.6114 .
- [20] Kodali, N., Abernethy, J., Hays, J., Kira, Z., 2017. On convergence and stability of gans. arXiv preprint arXiv:1705.07215 .
- [21] Kynkänniemi, T., Karras, T., Laine, S., Lehtinen, J., Aila, T., 2019. Improved precision and recall metric for assessing generative models. Advances in Neural Information Processing Systems 32.
- [22] Lin, Z., Sekar, V., Fanti, G., 2021. Why spectral normalization stabilizes gans: Analysis and improvements. Advances in neural information processing systems 34.

[23] Maas, A.L., Hannun, A.Y., Ng, A.Y., et al., 2013. Rectifier nonlinearities improve neural network acoustic models, in: Proc. icml, Citeseer, p. 3.

[24] Mao, X., Li, Q., Xie, H., Lau, R.Y., Wang, Z., Paul Smolley, S., 2017. Least squares generative adversarial networks, in: Proceedings of the IEEE international conference on computer vision, pp. 2794–2802.

[25] Mescheder, L., Geiger, A., Nowozin, S., 2018. Which training methods for gans do actually converge?, in: International conference on machine learning, PMLR, pp. 3481–3490.

[26] Miyato, T., Kataoka, T., Koyama, M., Yoshida, Y., 2018. Spectral normalization for generative adversarial networks. arXiv preprint arXiv:1802.05957.

[27] Miyato, T., Koyama, M., 2018. cgans with projection discriminator. arXiv preprint arXiv:1802.05637.

[28] Van den Oord, A., Kalchbrenner, N., Espeholt, L., Vinyals, O., Graves, A., et al., 2016. Conditional image generation with pixelcnn decoders. Advances in neural information processing systems 29.

[29] Park, S., Shin, Y.G., 2021a. Generative residual block for image generation. Applied Intelligence, 1–10.

[30] Park, S., Shin, Y.G., 2021b. A novel generator with auxiliary branch for improving gan performance. arXiv preprint arXiv:2112.14968.

[31] Park, S., Shin, Y.G., 2022. Generative convolution layer for image generation. Neural Networks.

[32] Park, S., Yeo, Y.J., Shin, Y.G., 2022a. Pconv: simple yet effective convolutional layer for generative adversarial network. Neural Computing and Applications 34, 7113–7124.

[33] Park, S., Yoo, C.H., Shin, Y.G., 2022b. Effective shortcut technique for generative adversarial networks. Applied Intelligence, 1–13.

[34] Reed, S., Akata, Z., Yan, X., Logeswaran, L., Schiele, B., Lee, H., 2016. Generative adversarial text to image synthesis. arXiv preprint arXiv:1605.05396.

[35] Ross, A., Doshi-Velez, F., 2018. Improving the adversarial robustness and interpretability of deep neural networks by regularizing their input gradients, in: Proceedings of the AAAI Conference on Artificial Intelligence, pp. 1660–1669.

[36] Roth, K., Lucchi, A., Nowozin, S., Hofmann, T., 2017. Stabilizing training of generative adversarial networks through regularization, in: Advances in neural information processing systems, pp. 2018–2028.

[37] Sagong, M.C., Shin, Y.G., Kim, S.W., Park, S., Ko, S.J., 2019. Pepsi: Fast image inpainting with parallel decoding network, in: Proceedings of the IEEE/CVF conference on computer vision and pattern recognition, pp. 11360–11368.

[38] Sagong, M.C., Yeo, Y.J., Shin, Y.G., Ko, S.J., 2022. Conditional convolution projecting latent vectors on condition-specific space. IEEE Transactions on Neural Networks and Learning Systems.

[39] Sajjadi, M.S., Bachem, O., Lucic, M., Bousquet, O., Gelly, S., 2018. Assessing generative models via precision and recall. Advances in neural information processing systems 31.

[40] Salimans, T., Goodfellow, I., Zaremba, W., Cheung, V., Radford, A., Chen, X., 2016. Improved techniques for training gans, in: Advances in neural information processing systems, pp. 2234–2242.

[41] Shin, Y.G., Sagong, M.C., Yeo, Y.J., Kim, S.W., Ko, S.J., 2020. Pepsi++: fast and lightweight network for image inpainting. IEEE Transactions on Neural Networks and Learning Systems.

[42] Szegedy, C., Vanhoucke, V., Ioffe, S., Shlens, J., Wojna, Z., 2016. Rethinking the inception architecture for computer vision, in: Proceedings of the IEEE conference on computer vision and pattern recognition, pp. 2818–2826.

[43] Van Oord, A., Kalchbrenner, N., Kavukcuoglu, K., 2016. Pixel recurrent neural networks, in: International conference on machine learning, PMLR, pp. 1747–1756.

[44] Wang, J., Yang, C., Xu, Y., Shen, Y., Li, H., Zhou, B., 2021. Improving gan equilibrium by raising spatial awareness. arXiv preprint arXiv:2112.00718.

[45] Wei, X., Gong, B., Liu, Z., Lu, W., Wang, L., 2018. Improving the improved training of wasserstein gans: A consistency term and its dual effect. arXiv preprint arXiv:1803.01541.

[46] Wu, B., Zhao, S., Chen, C., Xu, H., Wang, L., Zhang, X., Sun, G., Zhou, J., 2019. Generalization in generative adversarial networks: A novel perspective from privacy protection. arXiv preprint arXiv:1908.07882.

[47] Wu, Y.L., Shuai, H.H., Tam, Z.R., Chiu, H.Y., 2021. Gradient normalization for generative adversarial networks. arXiv preprint arXiv:2109.02235.

[48] Yeo, Y.J., Sagong, M.C., Park, S., Ko, S.J., Shin, Y.G., 2022. Image generation with self pixel-wise normalization. arXiv preprint arXiv:2201.10725.

[49] Yeo, Y.J., Shin, Y.G., Park, S., Ko, S.J., 2021. Simple yet effective way for improving the performance of gan. IEEE Transactions on Neural Networks and Learning Systems.

[50] Yu, F., Seff, A., Zhang, Y., Song, S., Funkhouser, T., Xiao, J., 2015. LSUN: Construction of a large-scale image dataset using deep learning with humans in the loop. arXiv preprint arXiv:1506.03365.

[51] Yu, J., Lin, Z., Yang, J., Shen, X., Lu, X., Huang, T.S., 2018. Free-form image inpainting with gated convolution. arXiv preprint arXiv:1806.03589.

[52] Yu, N., Liu, G., Dundar, A., Tao, A., Catanzaro, B., Davis, L.S., Fritz, M., 2021. Dual contrastive loss and attention for gans, in: Proceedings of the IEEE/CVF International Conference on Computer Vision, pp. 6731–6742.

[53] Zhang, H., Zhang, Z., Odena, A., Lee, H., 2019. Consistency regularization for generative adversarial networks. arXiv preprint arXiv:1910.12027.

[54] Zhao, Z., Singh, S., Lee, H., Zhang, Z., Odena, A., Zhang, H., 2020. Improved consistency regularization for gans. arXiv preprint arXiv:2002.04724.

[55] Zhu, J.Y., Park, T., Isola, P., Efros, A.A., 2017. Unpaired image-to-image translation using cycle-consistent adversarial networks, in: Proceedings of the IEEE international conference on computer vision, pp. 2223–2232.